tapraid4/zh4-ahea/zh4-ahea/zh400508/zh48209d08z | xppws | S=1 | 3/5/08 | 12:14 | MS: H-00986-2007 | Ini: 05/JTG/BEW

the Function of Human Body from the Ministry of Health, Labor and Welfare of Japan (H15-19 Physi-001) and by the Suzuken Memorial Foundation.

REFERENCES

1. **American Heart Association.** 2005 American Heart Association guidelines for cardiopulmonary resuscitation and emergency cardiovascular care: Part 7.5: Postresuscitation support. *Circulation* 112, *Suppl* IV: IV-84–IV-88, 2005.
2. **Bernard SA, Gray TW, Buist MD, Jones BM, Silvester W, Gutteridge G, Smith K.** Treatment of comatose survivors of out-of-hospital cardiac arrest with induced hypothermia. *N Engl J Med* 346: 557–563, 2002.
3. **Boddicker KA, Zhang Y, Zimmerman MB, Davies LR, Kerber RE.** Hypothermia improves defibrillation success and resuscitation outcomes from ventricular fibrillation. *Circulation* 111: 3195–3201, 2005.
4. **Bukauskas FF, Weingart R.** Temperature dependence of gap junction properties in neonatal rat heart cells. *Pflügers Arch* 423: 133–139, 1993.
5. **Bursac N, Tung L.** Acceleration of functional reentry by rapid pacing in anisotropic cardiac monolayers: formation of multi-wave functional reentries. *Cardiovasc Res* 69: 381–389, 2006.
6. **Cavalie A, McDonald TF, Pelezer D, Trautwein W.** Temperature-induced transitory and steady-state changes in the calcium current of guinea pig ventricular myocytes. *Pflügers Arch* 405: 294–296, 1985.
7. **Chorro FJ, Guerrero J, Ferrereo A, Tormos A, Mainar L, Millet J, Canoves J, Porres JC, Sanchis J, Lopez-Merino V, Such L.** Effects of acute reduction of temperature on ventricular fibrillation activation patterns. *Am J Physiol Heart Circ Physiol* 283: H2331–H2340, 2002.
8. **Davidenko JM, Salmonsz R, Pertsov AM, Baxter WT, Jalife J.** Effects of pacing on stationary reentrant activity. *Circ Res* 77: 1166–1179, 1995.
9. **Efimov IR, Cheng Y, Van Wagoner DR, Mazgalev T, Tchou PJ.** Virtual electrode-induced phase singularity: a basic mechanism of defibrillation failure. *Circ Res* 82: 918–925, 1998.
10. **Gambassi G, Cerbai E, Pahor M, Capogrossi MC, Carbonin P, Mugelli A.** Temperature modurates calcium homeostasis and ventricular arrhythmias in myocardial preparations. *Cardiovasc Res* 28: 391–399, 1994.
11. **Gray RA.** Global mechanisms of defibrillation. In: *Cardiac Electrophysiology: from Cell to Bedside* (4th ed.), edited by Zipes DP and Jalife J. Philadelphia, PA: Saunders, 2004, p. 417–425.
12. **Gray RA, Pertsov AM, Jalife J.** Spatial and temporal organization during cardiac fibrillation. *Nature* 392: 75–78, 1998.

AQ: 5 12a. **Hypothermia after Cardiac Arrest Study Group.** Mild therapeutic hypothermia to improve the neurologic outcome after cardiac arrest. *N Engl J Med* 346: 549–556, 2002.

13. **Kirsch GE, Sykes JS.** Temperature dependence of Na^+ currents in rabbit and frog muscle membranes. *J Gen Physiol* 89: 239–251, 1987.
14. **Kiyosue T, Arita M, Muramatsu H, Spindler AJ, Noble D.** Ionic mechanisms of action potential prolongation at low temperature in guinea-pig ventricular myocytes. *J Physiol* 468: 85–106, 1993.
15. **Koller ML, Riccio ML, Gilmour RF Jr.** Dynamic restitution of action potential duration during electrical alternans and ventricular fibrillation. *Am J Physiol Heart Circ Physiol* 275: H1635–H1642, 1998.
16. **Lee MH, Lin SF, Ohara T, Omichi C, Okuyama Y, Chudin E, Garfinkel A, Weiss JN, Karagueuzian HS, Chen PS.** Effects of diacetyl monoxime and cytochalasin D on ventricular fibrillation in swine right ventricles. *Am J Physiol Heart Circ Physiol* 280: H2689–H2696, 2001.
17. **Marion DW, Leonov Y, Ginsberg M, Katz LM, Kochanek PM, Lechleuthner A, Nemoto EM, Obrist W, Safar P, Sterz F, Tisherman SA, White RJ, Xiao F, Zar H.** Resuscitative hypothermia. *Crit Care Med* 24: S81–S89, 1996.
18. **Mortensen E, Berntsen R, Tveita T, Lathrop DA, Refsum H.** Changes in ventricular fibrillation threshold during acute hypothermia. A model for future studies. *J Basic Clin Physiol Pharmacol* 4: 313–319, 1993.
19. **Noujaim S, Pandit SV, Berenfeld O, Vikstrom K, Cerrone M, Minonov S, Zugermayr M, Lopatin AN, Jalife J.** Up-regulation of the inward rectifier K^+ current (I_{K1}) in the mouse heat accelerates and stabilizes rotors. *J Physiol* 578: 315–326, 2007.
20. **Qu Z.** Critical mass hypothesis revisited: role of dynamical wave stability in spontaneous termination of cardiac fibrillation. *Am J Physiol Heart Circ Physiol* 290: H255–H263, 2006.
21. **Salama G, Kanai AJ, Huang D, Efimov IR, Girouard SD, Rosenbaum DS.** Hypoxia and hypothermia enhance spatial heterogeneities of repolarization in guinea pig hearts: analysis of spatial autocorrelation of optically recorded action potential durations. *J Cardiovasc Electrophysiol* 9: 164–183, 1998.
23. **Ujihelyi MR, Sims JJ, Dubin SA, Vender J, Miller AW.** Defibrillation energy requirements and electrical heterogeneity during total body hypothermia. *Crit Care Med* 29: 1006–1011, 2001.
24. **Weiss JN, Qu Z, Chen PS, Lin SF, Karagueuzian HS, Hayashi H, Garfinkel A, Karma A.** The dynamics of cardiac fibrillation. *Circulation* 112: 1232–1240, 2005.
25. **Wu TJ, Lin SF, Weiss JN, Ting CT, Chen PS.** Two types of ventricular fibrillation in isolated rabbit hearts importance of excitability and action potential duration restitution. *Circulation* 106: 1859–1866, 2002.
26. **Yamazaki M, Honjo H, Nakagawa H, Ishiguro YS, Okuno Y, Sakuma I, Kamiya K, Kodama I.** Mechanisms of destabilization and early termination of spiral wave reentry in the ventricle by a class antiarrhythmic agent, nifekalant. *Am J Physiol Heart Circ Physiol* 292: H539–H548, 2007.

Journal of NeuroEngineering and Rehabilitation

BioMed Central

Research

Open Access

A pilot study on pupillary and cardiovascular changes induced by stereoscopic video movies

Hiroshi Oyamada[1], Atsuhiko Iijima[1], Akira Tanaka[2], Kazuhiko Ukai[3], Haruo Toda[1], Norihiro Sugita[4], Makoto Yoshizawa[4] and Takehiko Bando*[1]

Address: [1]Division of Integrated Physiology, Niigata University Graduate School for Medical and Dental Sciences, Asahi-machi1, Niigata, 951-8510, Japan, [2]Department of Human Support System, Faculty of Symbiotic Systems Science, Fukushima University, Fukushima, Japan, [3]Department of Applied Physics, Waseda University, Tokyo, Japan and [4]Research Division on Advanced Information Technology, Information Synergy Center, Tohoku University, Sendai, Japan

Email: Hiroshi Oyamada - theta@qg7.so-net.ne.jp; Atsuhiko Iijima - a-iijima@med.niigata-u.ac.jp; Akira Tanaka - a-tanaka@sss.fukushima-u.ac.jp; Kazuhiko Ukai - ukai@waseda.jp; Haruo Toda - toda@med.niigata-u.ac.jp; Norihiro Sugita - sugita@yoshizawa.ecei.tohoku.ac.jp; Makoto Yoshizawa - yoshizawa@yoshizawa.ecei.tohoku.ac.jp; Takehiko Bando* - bando@adm.niigata-u.ac.jp

* Corresponding author

Published: 4 October 2007

Journal of NeuroEngineering and Rehabilitation 2007, **4**:37 doi:10.1186/1743-0003-4-37

Received: 1 June 2006
Accepted: 4 October 2007

This article is available from: http://www.jneuroengrehab.com/content/4/1/37

Abstract

Background: Taking advantage of developed image technology, it is expected that image presentation would be utilized to promote health in the field of medical care and public health. To accumulate knowledge on biomedical effects induced by image presentation, an essential prerequisite for these purposes, studies on autonomic responses in more than one physiological system would be necessary. In this study, changes in parameters of the pupillary light reflex and cardiovascular reflex evoked by motion pictures were examined, which would be utilized to evaluate the effects of images, and to avoid side effects.

Methods: Three stereoscopic video movies with different properties were field-sequentially rear-projected through two LCD projectors on an 80-inch screen. Seven healthy young subjects watched movies in a dark room. Pupillary parameters were measured before and after presentation of movies by an infrared pupillometer. ECG and radial blood pressure were continuously monitored. The maximum cross-correlation coefficient between heart rate and blood pressure, ρ_{max}, was used as an index to evaluate changes in the cardiovascular reflex.

Results: Parameters of pupillary and cardiovascular reflexes changed differently after subjects watched three different video movies. Amplitudes of the pupillary light reflex, CR, increased when subjects watched two CG movies (movies A and D), while they did not change after watching a movie with the real scenery (movie R). The ρ_{max} was significantly larger after presentation of the movie D. Scores of the questionnaire for subjective evaluation of physical condition increased after presentation of all movies, but their relationship with changes in CR and ρ_{max} was different in three movies. Possible causes of these biomedical differences are discussed.

Conclusion: The autonomic responses were effective to monitor biomedical effects induced by image presentation. Further accumulation of data on multiple autonomic functions would contribute to develop the tools which evaluate the effects of image presentation to select applicable procedures and to avoid side effects in the medical care and rehabilitation.

Introduction

Taking advantage of recent developments in the image technology, new trials of efforts to promote health by utilizing images are expected. Images may be applied to the medical care, or may be used as the tools to monitor the effects of the care. One of the prerequisite of these trials is the understanding of biomedical influences evoked by visual stimulation. The biomedical influences evoked by presentation of images have been studied in efforts to prevent biomedical hazards such as asthenopia and other symptoms of the VDT syndrome evoked by using video displays in the business offices [1-6]. Results of these studies indicated that autonomic responses, including cardiovascular and ocular responses, would provide valuable information.

In this study, changes in the pupillary light reflex and cardiovascular reflex evoked by watching three different stereoscopic video movies were measured in healthy young subjects, and related with the subjective assessment of discomfort measured as scores of the questionnaire collected at the same time. It is shown that biomedical effects evoked by presentation of video movies were different depending on the properties of video movies. Possible causes of these differences are discussed. Accumulation of the knowledge may provide the efficient tool to select proper images applicable to the cases, and to evaluate properly the effects of treatments in the field of medical care and rehabilitation. Such estimation is also necessary to avoid the side effect or aggravation due to improper stimuli. Some of the preliminary data were reported in the abstract form [7].

Methods

Subjects

Subjects were seven (five male and two female) medical students (23.0 ± 0.9 years). The procedures and general purpose of the experiments were explained to subjects, but no information on the expected results was given. The Bioethics Committee of the Niigata University School of Medicine approved the experiments in this study, and all subjects gave the informed consents to participate in the study.

Presentation of motion pictures

Three stereoscopic movies of 5-min-long were used as the test stimuli. The digital signals of the movies were fed to a liquid-crystalline display, and total brightness of a frame in the movie was monitored by a photocell on the screen, which was positioned in front of the display. The binocular disparity was roughly evaluated by the MATLAB software (MathWorks, Inc), in which the separation of the central objects in even and odd frames of the movie was calculated.

Among three movies, two were made of computer graphics (CG), and the other was the real scenery taken by a camera in a car of the roller coaster (R), which gave strong vection sensation in all subjects, probably because the quick changes in the apparent velocities of objects in the scenery would invoke the past experiences of subjects. One of the CG movies was an imaginary work, in which various objects were moving violently without a consistent story through the movie (movie A). The other CG movie dealt with an imaginary ancient world in which many kinds of dinosaurs approached the subjects with the progression of the story, and finally the subject was attacked by a tyrannosaurus (movie D).

Other properties of the movies were as follows. Firstly, brightness in two CG (A and D) movies was changed frequently. Their mean brightness was in the same range, but switching in the brightness was much frequent in the movie D. The movie R had stable and high brightness. Secondly, the degree of binocular disparity is larger in two CG movies (largest in the movie D) than in the movie R. Thirdly movies D and R had a kind of story, which proceeded from the beginning to the end, while blocks of frames were not temporally continuous in the movie A.

Subjects watched three different video images in a random order in a day. Before the presentation of each video movie, five minutes of rest were allowed for each subject, which were necessary to prepare the stable condition of subjects, and to collect stable cardiovascular data as the control. Just after presentation of the movie, measurement of pupillary parameters was quickly performed. Then, five minutes of the rest were again allowed to collect cardiovascular data. The same subjects repeated the experiments within two weeks at the corresponding time zone in each day to avoid the influence of the circadian rhythm of pupillary parameters [8].

Stereoscopic movies in digital video cassettes were consisted with the sequential frames of odd and even fields, which provided images to the left and right eyes with the binocular disparity necessary for stereoscopic vision. They were replayed by a video cassette recorder (WV-D10000, Sony Co.), fed to a signal distributor, and then were rear-projected by two aligned liquid-crystalline display (LCD) projectors (TH-L795J, Matsushita Elec. Co., XGA, total of 1400 lm) onto an 80-inch screen (Fig. 1). By an electronic distributor, even and odd fields of the images were allotted to each of the two LCD projectors. Each of two projectors had a polarizing filter, orthogonal to each other. Subjects sat in a chair at 2 m from the screen, wearing polarizing-glasses and watching motion pictures in the 80-inch screen, with the comfortable posture in the dark room (illuminance, 10 l× at the floor of the room just in front of the screen). The size of the images in the screen

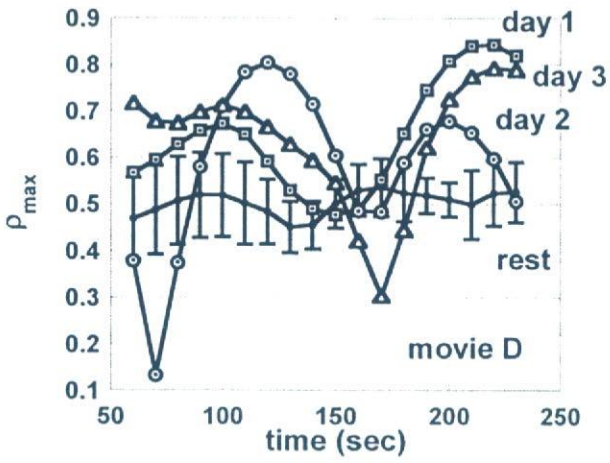

Figure 1
The ρ_{max} of a subject obtained in the consecutive three days (day 1, day 2 and day 3) during video presentation of the movie D is shown respectively. The mean and SE of ρ_{max} obtained in the rest before and after presentation of the movies $\rho_{max\_control}$ are also shown (control, n = 6).

was 120 cm (length) × 160 cm (width). The visual angle was vertically 17 deg, and horizontally 22 deg, because the distance between the subject and the screen was 2 m.

Measurement of pupil diameter

Pupil diameters were measured by an infrared pupillometer (Iriscorder C7364, Hamamatsu Photonics Co.), in which a charge-coupled device (CCD) camera took the image of a pupil with a sampling rate of 1/60 sec. This camera had an effective field of 30 mm × 22.5 mm. The field was illuminated by a light-emitting diode (LED) with a peak wavelength of 890 nm. Another LED in the pupillometer (peak wavelength, 660 nm; maximum intensity, 10 μW) was lit for 1 sec to induce the pupillary light reflex. Measurements of the pupil were performed in the dark room (illuminance, 10 lx). In the control, the parameters of the pupil were measured after the rest of 5 min in the dark room. After presentation of movies, they were measured just after presentation in the dark room. Then the difference in the brightness of video movies might contribute to the differences in the pupillary parameters, but it was not the case in this study (see Discussion, changes in pupillary parameters). Data were collected by an interface (PCI-MIO-16XE-10, National Instruments Co.) by the aid of the LabVIEW (National Instruments Co.) and stored in a hard disk. Original data were also stored in a digital tape by using a data-recorder (RD135T, TEAC Co.).

A polynomial curve was fitted to the rising or falling time course of the pupillary light responses. The maximal velocity and acceleration of pupillary constriction, and the maximal velocity of re-dilation of the pupil in the light reflex were calculated by the first- and second-order differentiation of the fitted curve.

Amplitudes of the pupillary light reflex are dependent on the pupil diameter before light stimulation (baseline pupil diameter, D1). We then adopted the constriction ratio [9], CR, to balance the differences in D1 as follows: CR = (D1–D2)/D1, where D2 was the diameter of the pupil at the peak of the light reflex. The CR_{ratio} was defined as (CRaf/CRbf), to evaluate the changes in CR before (CRbf) and after (CRaf) presentation of movies.

Measurement of blood pressure and ECG

ECG (electrocardiogram) (Nihon-Koden Co.) and radial blood pressure (JENTOW770, Colin Japan Co.) were continuously collected by a data-collection system at a sampling rate of 1 kHz with 12 bit resolution. Data in the rest time before and after video presentation (5 min each), and those during video presentation (5 min) were analyzed. Heart rate (min^{-1}) was calculated from the reciprocal of the inter-R-wave interval of the ECG signal. Mean blood pressure (mmHg) was obtained as the mean value of the pressure signal over one heartbeat. Beat-to-beat mean pressure and heart rate were interpolated by a cubic spline function and were re-sampled every 0.469 sec to yield corresponding beat-to-beat data, denoted by *BP* and *HR*, respectively. The data is filtered through a band-pass filter with the bandwidth between 0.08 Hz and 0.12 Hz to extract Mayer wave components. At time t, Hanning window whose interval is $[t\text{-}60, t\text{+}60]$ in second is used to segment *BP* and *HR* into 2 min-long data. After this processing, the normalized cross-correlation function $\rho(\tau)$ between *BP* and *HR* is calculated. The ρ_{max} was defined as the maximum cross-correlation coefficient $\rho(\tau)$ for the positive τ [10,11]. The ρ_{max} would be 1, if changes in the heart rate depend completely on changes in blood pressure. But it is ordinarily lower than 1, because the heart rate depends also on the biological noises embedded in the baroreflex loop. When noises are increased, for example, by emotional inputs, ρ_{max} is lowered. The ρ_{max} would be also lowered, if the vascular resistance changes without the corresponding change in pulse rate. On the other hand, increased ρ_{max} would be induced by the reduction of biological noises. The contribution of noises may be lowered by the stimuli that drive cardiac reactions to prepare movements of the body.

Data analysis

Subjects evaluated their physical conditions during the rest before and after presentation of movies by filling out

a questionnaire with 10 items on a seven-point rating scale [12].

We used the paired *t*-test (two tailed) to compare means. Pearson's correlation coefficient was used to assess the relationship between two parameters. We used the SPSS software (release 10.07J, SPSS, Inc.) for statistical analyses.

Results

The scores of the questionnaire (the last column in Table 1) increased significantly after the subjects watched any of three video movies ($p < 0.02$, for movie D, and $p < 0.05$, for movie A and R, paired *t*-test), indicating that they felt some discomforts by watching 3D movies or possibly by restriction of body movement with various equipments in the experiment.

Pupillary parameters

Seven subjects watched three different video movies in a random order in a day, and the test was repeated two times within two weeks. Then total of 21 trials for each of three movies was performed. The changes in data obtained in the day1, day2 and day3 were not different each other (ANOVA, LSD and Bonferroni), and therefore, data in these 21 trials were pooled. The baseline pupil diameters (D1) were measured just before the onset of light stimulus which induced the pupillary light reflex. The D1_video, which was obtained after presentation of video movies, was significantly smaller than the D1_control, which obtained before presentation in all of three movies (Table 1). In addition, values of the D1_video for any of three video movies were not significantly different each other. The pupil diameters at the peak of the light reflex (D2) were also significantly smaller after presentation of movies.

The constriction ratio of the light reflex, CR, was significantly larger after presentation of the movies D ($p < 0.01$, paired *t*-test) and A ($p < 0.05$) than the control obtained before presentation (the control) (Table 1), while after presentation of the movie R the CR was not significantly different from the control ($p > 0.05$). Other parameters of the pupillary light reflex, i.e., the latency of the constriction, the velocity of constriction (vc), the velocity of redilation (vd), the acceleration of constriction (ac), and the time at the peak of constriction (peak time) were not significantly different before and after presentation of movies A, D and R.

Cardiovascular reflex

Heart rate and blood pressure were continuously monitored. The ρ_{max} was calculated for 2 min. Then the data window was shifted by 10 seconds, and the ρ_{max} was again calculated. In this way, 18 points of the ρ_{max} were obtained between 60 and 230 seconds following the onset of the movie. In Fig. 1, the values of the ρ_{max} measured when a subject watched movie D in the first, second and third days are plotted against the time after the onset of the movie.

To evaluate the changes in the ρ_{max}, the ρ_{max_ratio} was defined. Firstly the ρ_{max} at each of the 18 points along the time following the onset of a movie was calculated (ρ_{max_test}). Secondly the values of ρ_{max} at the corresponding points in the rest before and after presentation were averaged ($\rho_{max\_control}$). The standardized ρ_{max} is defined as the $\rho_{max\_test}/\rho_{max\_control}$ at each of 18 points. Thirdly the mean of the standardized ρ_{max} for 18 points gave the ρ_{max_ratio}. In Table 2, the mean $\rho_{max\_control}$, the mean ρ_{max_test} as well as the ρ_{max_ratio} are shown. The mean ρ_{max_test} was significantly larger than the mean $\rho_{max\_control}$ when the subject watched the movie D ($p < 0.05$, paired *t*-test), while the mean values of the ρ_{max_test} were not significantly different after presentation of movies A and R ($p > 0.05$).

Correlation between objective and subjective indices

The CR_{ratio} obtained after the subject watched movie D or R was correlated significantly with the difference in the scores of questionnaire ($p < 0.01$) (Table 3, Pearson's coefficient of correlation, n = 21, and Fig. 2B–C), while after presentation of the movie A, they were not correlated significantly ($p > 0.05$) (Fig. 2A). Increased discomfort after presentation of movies is indicated as the positive values

Table 1: The pupil parameters and the scores of questionnaire obtained before (control) and after presentation of movies A, D and R

	D1 [mm]	D2 [mm]	CR	latency [msec]	vc [mm/sec]	vd [mm/sec]	ac [mm/sec2]	peak time [sec]	score of questionnaire
Control	6.62 ± 0.89	5.25 ± 1.03	0.21 ± 0.07	303 ± 29	3.99 ± 1.29	1.14 ± 0.36	32.1 ± 11.3	1.10 ± 0.24	32.4 ± 10.2
movie A	5.95 ± 0.98**	4.48 ± 1.06**	0.25 ± 0.09*	304 ± 28	4.33 ± 1.27	1.14 ± 0.42	34.8 ± 12.7	1.10 ± 0.27	36.1 ± 10.3*
movie D	6.08 ± 0.92**	4.54 ± 0.93**	0.26 ± 0.08**	300 ± 32	4.35 ± 1.11	1.16 ± 0.48	32.3 ± 9.6	1.10 ± 0.20	38.0 ± 14.1**
movie R	6.15 ± 0.86**	4.77 ± 0.92**	0.23 ± 00.8	306 ± 33	4.02 ± 1.37	1.10 ± 0.43	32.2 ± 11.5	1.06 ± 0.18	36.7 ± 11.3*

mean ± SD. D1: baseline pupil diameter just before light stimulation to induce the light reflex (mm), D2: pupil diameter at the peak of the light reflex (mm), CR: the amplitude of the pupillary light reflex (D1–D2) divided by D1, latency: the latency of the pupillary light reflex (msec), vc: the velocity of constriction (mm/sec), vd: the velocity of redilation (mm/sec), ac: the acceleration of the constriction (mm/sec^2), peak time: time at the peak of the pupillary light reflex (sec), and the scores of the questionnaire. *, $p < 0.05$, **, $p < 0.01$. Paired *t*-test (two-tailed).

Table 2: Mean values of $\rho_{max\_control}$, ρ_{max_test}, and ρ_{max_ratio} are shown for each video movie (movie A, D and R)

	$\rho_{max\_control}$	ρ_{max_test}	ρ_{max_ratio}
Movie A	0.65 ± 0.10	0.66 ± 0.13	1.03± 0.06
Movie D	0.66 ± 0.12	0.70 ± 0.08*	1.11± 0.05
Movie R	0.66 ± 0.09	0.69 ± 0.12	1.08± 0.07

mean ± SD. *, $p < 0.05$. Paired *t*-test.

of the differences in scores of the subjective evaluation in Fig. 2.

The correlation of the ρ_{max_ratio} with the difference in the scores of questionnaire was not significant when the subjects watched any of three movies ($p > 0.05$) (Fig. 2D–F, and Table 4). In addition, the CR_{ratio} was not correlated with the ρ_{max_ratio} ($p > 0.05$) (Table 5).

Discussion

Changes in pupillary parameters

The diameter of the pupil is controlled both by sympathetic and parasympathetic activities [13]. Pupil is constricted by increased contraction of the pupillary constrictor muscle, which is innervated by parasympathetic short ciliary and oculomotor nerves, and/or by decreased tension of the pupillary dilator muscles, innervated by sympathetic nerves. The parasympathetic oculomotor neurons are in the dorso-rostral oculomotor nucleus in the midbrain. Sympathetic innervation is originated from the cervical and superior thoracic segments of the spinal cord. Changes in pupillary size may reflect the balance of sympathetic and parasympathetic tones, and are the good measure of the sustained state of the autonomic function. On the other hand, the pupillary light reflex is controlled through the arc through the retinal ganglion cells, the pretectum, and the parasympathetic oculomotor neurons. Changes in parameters of the pupillary light reflex depend probably on the activation levels of the brain stem structures related to this reflex arc.

In point of view of the sustained autonomic function, it is suggested that parasympathetic tone prevailed over sympathetic tone after presentation of any of three movies, because baseline pupillary sizes were decreased (Table 1).

Table 3: Correlation coefficient (Pearson) between CR_{ratio} and differences in the scores of questionnaire

	correlation coefficient	level of significance
movie A	0.059	0.799
movie D	-0.567**	0.007
movie R	-0.590**	0.005

**, $p < 0.01$. In the second column, the levels of significance are shown.

The miotic condition may be caused by the relaxed condition of the subject after the end of the task, by the fatigue or by the drowsiness in the dark room, although no subject reported sleepiness in the experiment. On the other hand, CR, which is the change in the amplitude of the light reflex, was different, depending on the movies. The CR increased significantly after presentation of two CG movies, and the change was not significant after presentation of the movie R (Tables 1). Because changes in baseline pupil diameters were not significantly different among three movies, the differences in CR were not dependent on the mean brightness of movies, and other causes should be sought. By comparing properties of three movies (Material and Methods, presentation of motion pictures), changes in the CR might be induced by accumulation of the activities in the brain stem possibly due to the unnatural changes in the disparity and/or brightness, which could facilitate the transmission of the visual signals to the intraocular sphincter muscles.

Changes in the cardiovascular reflex

Cardiovascular measures, such as spectral analyses of the R-R interval in the cardiac rhythm [14-16], have been typical tools to evaluate the autonomic nervous function. However, in these traditional methods, only slight body movement was allowed. By newly developed index, the ρ_{max}, stable measurement of parameters of the cardiovascular reflex is possible when the subjects watch movies with less severe restriction of body movement.

The ρ_{max} was increased significantly after presentation of the movie D. In movie D, subjects were met various dinosaurs one after another and were attacked by some of them, which drove cardiac reactions to escape from them. Such reactions could increase the contribution of the baroreflex over biological noises (see Materials and Methods, measurement of blood pressure and ECG), which might increase ρ_{max}.

Correlation among the pupillary, cardiovascular and subjective indices

In order to relate the subjective and objective evaluation of biomedical effects induced by presentation of images, changes in the CR and ρ_{max} were related with the differences in the scores of questionnaire. Differences in the subjective evaluation correlated significantly with changes in CR after presentation of movies D and R, but in other combinations the correlation was not significant ($p > 0.05$).

The different relation to the subjective evaluation of the pupillary light reflex and the baroreflex would suggest that different factors contributed to the biomedical influences caused by image presentation. Although further studies with larger number of subjects are necessary, it is sug-

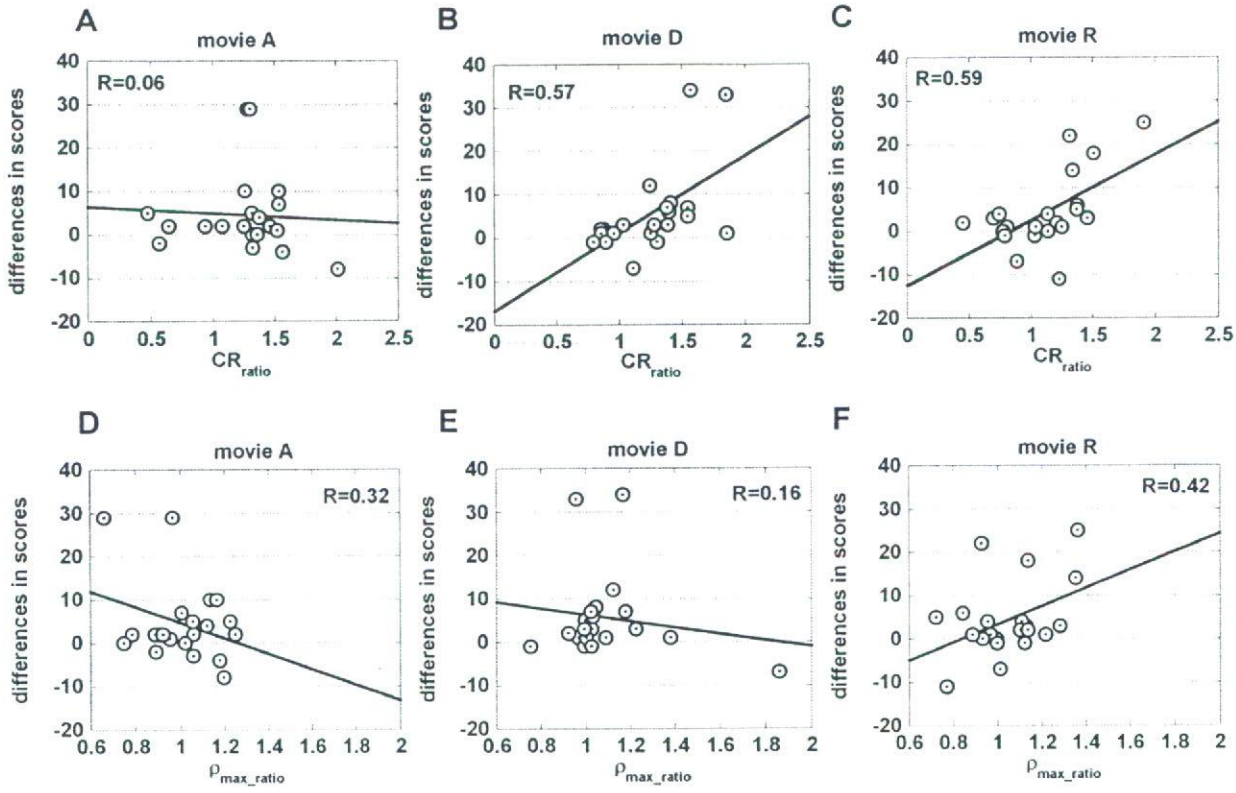

Figure 2
Correlation of pupil and cardiovascular parameters with the scores of questionnaire. A-C. Correlation of CR_{ratio} with the differences in the scores of questionnaire when subjects watched the movies A, D and R, respectively, are shown. D-F. Correlation of ρ_{max_ratio} with the differences in the scores of questionnaire when subjects watched the movies A, D and R, respectively, are shown.

gested that biomedical influences should be evaluated by multiple physical parameters, which are carefully selected.

Significance of the present study

Pupillary and cardiovascular parameters as well as subjective evaluation were changed after image presentation, and the effects were different depending on the types of images. The results may be utilized to detect subtle changes in physical parameters to assess the effect of medical care [17,18]. Images can also be used as the tool for the treatment, for example, of the patients with panic disorder [19]. Images should be carefully selected, however, and the biomedical effects must be carefully monitored to avoid side effects or aggravation. Rehabilitation of posture and movement of paralyzed patients may be facilitated in virtual environment which would promote their motivation, but some patients may complain of cybersickness due to the virtual motion scenery. Tools to monitor bio-

Table 4: Correlation coefficient (Pearson) between ρ_{max_ratio} and differences in the scores of questionnaire. In the second column, the levels of significance are shown

	correlation coefficient	level of significance
movie A	032	0.161
movie D	0.16	0.491
movie R	-0.42	0.059

Table 5: Correlation coefficient (Pearson) between ρ_{max_ratio} and CR_{ratio}. In the second column, the levels of significance are shown

	correlation coefficient	level of significance
movie A	0.07	0.77
movie D	0.11	0.65
movie R	0.21	0.37

medical influences are also needed, which are provided by monitoring parameters such as shown in the present study.

Although many questions remained to be clarified, this study is an important step to accumulate knowledge on biomedical effects evoked by audiovisual stimulation. By accumulation of such knowledge, the efficient tools would be developed to select proper images applicable to the medical care and rehabilitation, and to monitor undesirable effect of images to avoid side effect.

Acknowledgements

This work was partly supported by the Mechanical Social Systems Foundation, Japan Electronics and Information Technology Industries Association, Japan KEIRIN Association, the Ministry of Education, Science and Sports, and the Ministry of Economy, Trade and Industry. Written consent for publication was obtained from the subjects. We thank Michiko Kimishima for valuable help in project managements, and Junko Takahashi in secretarial assistance.

References

1. Saito M, Tanaka T, Oshima M: **Eyestrain in inspection and clerical workers.** *Ergonomics* 1981, **24:**161-173.
2. Gur S, Ron S, Heicklen-Klein A: **Objective evaluation of visual fatigue in VDU workers.** *Occup Med (Lond)* 1994, **44(4):**201-204.
3. Saito S, Sotoyama M, Saito S, Taptagaporn S: **Physiological indices of visual fatigue due to VDT operation: pupillary reflexes and accommodative responses.** *Ind Health* 1994, **32(2):**57-66.
4. Hasebe H, Oyamada H, Ukai K, Toda H, Bando T: **Changes in oculomotor functions before and after loading of a 3-D visually-guided task by using a head-mounted display.** *Ergonomics* 1996, **39:**1330-1343.
5. Ukai K, Tsuchiya K, Ishikawa S: **Induced pupillary hippus following near vision: increased occurrence in visual display unit workers.** *Ergonomics* 1997, **40:**1201-1211.
6. Takagi M, Abe H, Toda H, Usui T: **Accommodative and pupillary responses to sinusoidal target depth movement.** *Ophthalmic Physiol Opt* 1993, **13(3):**253-257.
7. Bando T, Oyamada H, Fukasaku S, Tanaka A, Yoshizawa M, Ukai K: **Changes in autonomic functions and subjective evaluation of physical conditions by three different types of stereoscopic video movies. [abstract].** *Jpn J Physiol* 2002, **52(Suppl):**S175.
8. Wilhelm B, Giedke H, Lüdtke H, Bittner E, Hofmann A, Wilhelm H: **Daytime variations in central nervous system activation measured by a pupillographic sleepiness test.** *J Sleep Res* 2001, **10(1):**1-7.
9. Hasegawa S, Ishikawa S: **Age changes in pupillary light reflex. A demonstration by means of a pupillometer.** *Nippon Ganka Gakkai Zasshi* 1989, **93(10):**955-961.
10. Sugita N, Yoshizawa M, Tanaka A, Abe K, Chiba S, Yambe T, Nitta S: **Quantitative evaluation of the effect of visually-induced motion sickness using causal coherence function between blood pressure and heart rate.** *Conf Proc IEEE Eng Med Biol Soc* 2004, **4:**2047-2410.
11. Yoshizawa M, Sugita N, Tanaka A, Masuda T, Abe K, Chiba S, Yambe T, Nitta S: **Assessment of emotional reaction induced by visual stimulation based on cross-correlation between pulse wave transmission time and heart rate in the Mayer wave-band.** *Conf Proc IEEE Eng Med Biol Soc* 2004, **4:**2411-2414.
12. Ando T, Tanaka A, Fukasaku S, Takada R, Okada M, Ukai K, Shizuka K, Oyamada H, Toda H, Taniyama T, Usui T, Yoshizawa M, Kiryu T, Takagi M, Saida S, Bando T: **Pupillary and cardiovascular responses to a video movie in senior human subjects.** *Auton Neurosci* 2002, **97(2):**129-135.
13. Brodal A: **The light reflex in "Neuronal Anatomy".** 3rd edition. Oxford Univ Press, New York; 1981:561-564.
14. Akselrod S, Gorden D, Madwed JB, Snidman NC, Shannon DC, Cohen RJ: **Hemodynamic regulation: investigation by spectral analysis.** *Am J Physiol* 1985, **249(4 Pt 2):**H867-H875.
15. Montano N, Ruscone TG, Porta A, Lombardi F, Pagani M, Malliani A: **Power spectrum analysis of heart rate variability to assess the changes in sympathovagal balance during graded orthostatic tilt.** *Circulation* 1994, **90:**1826-1831.
16. Pagani M, Federico L, Stefano G, Ornella R, Raffaello F, Paolo S, Giulia P, Gabriella M: **Power spectral analysis of heart rate and arterial pressure variabilities as a marker of sympatho-vagal interaction in man and conscious dog.** *Circulation Res* 1986, **59:**178-193.
17. Kojima M, Shioiri T, Hosoki T, Kitamura H, Bando T, Someya T: **Pupillary light reflex in panic disorder. A trial using audiovisual stimulation.** *Eur Arch Psychiatry Clin Neurosci* 2004, **254(4):**242-244.
18. Shioiri T, Kojima-Maruyama M, Hosoki T, Kitamura H, Tanaka A, Bando T, Someya T: **Dysfunctional baroreflex regulation of sympathetic nerve activity in remitted patients with panic disorder. A new methodological approach.** *Eur Arch Psychiatry Clin Neurosci* 2005, **255(5):**293-298.
19. Rothbaum BO, Hodges L, Anderson PL, Price L, Smith S: **Twelve-month follow-up of virtual reality and standard exposure therapies for the fear of flying.** *J Consult Clin Psychol* 2002, **70(2):**428-432.

Circ J 2007; **Suppl A:** A-26–A-31

Modulation of Spiral Wave Reentry by K^+ Channel Blockade

Haruo Honjo, MD; Masatoshi Yamazaki, MD;
Kaichiro Kamiya, MD; Itsuo Kodama, MD

It is well established that spiral wave reentry is the primary mechanism of ventricular tachyarrhythmias (ventricular fibrillation/tachycardia, VF/VT), but information is still limited concerning pharmacological modification of spiral waves by ion channel blockers. In this brief review, the antiarrhythmic and proarrhythmic actions of K^+-channel blockade (I_{Kr} and I_{K1}) are discussed in terms of spiral wave dynamics, primarily based on recent experimental findings in ventricular preparations perfused in vitro with the aid of high-resolution optical mapping, as well as their related theoretical studies using computer simulation. (*Circ J* 2007; **Suppl A:** A-26–A-31)

Key Words: Antiarrhythmic drugs; K^+ channel; Spiral wave reentry; Ventricular fibrillation/tachycardia

Ventricular tachyarrhythmias, including ventricular fibrillation (VF) and polymorphic ventricular tachycardia (VT), are the leading causes of sudden cardiac death. Recent theoretical studies using computer simulation on nonlinear excitable media and experimental studies using high-resolution optical mapping have revealed that spiral wave reentry rotating around a functional obstacle is the major mechanism underlying most of these tachyarrhythmias[1–14] In order to establish reliable therapeutic methods of effective prevention and termination of these tachyarrhythmias, better understanding of spiral waves in cardiac tissues is essential. However, information obtained from real hearts of animals or human patients is still limited, especially concerning pharmacological modulation of spiral wave dynamics, and findings provided by computer simulation studies remain to be validated.

Recently, the effects of nifekalant, a selective blocker of the rapid component of the delayed rectifier K^+ current (I_{Kr}), have been investigated in a 2-dimensional (2-D) layer of rabbit ventricular myocardium, using an original high-resolution video imaging system[15–17] It was found that nifekalant promotes self-termination of ventricular tachyarrhythmias through destabilization of spiral waves. In clinical practice, intravenous nifekalant is reported to be highly effective in terminating and preventing VT/VF that is resistant to other antiarrhythmic drugs and DC shocks[18,19] On the other hand, it is well known that excessive prolongation of ventricular action potentials by K^+-channel blockers (drug-induced QT prolongation) leads to an induction of torsades de pointes (TdP)-type polymorphic VT[20] In this brief review, such bimodal actions, antiarrhythmic and proarrhythmic, of K^+-channel blockers are discussed in terms of modulation of the spiral wave dynamics.

(Received February 21, 2007; accepted February 28, 2007)
Department of Cardiovascular Research, Research Institute of Environmental Medicine, Nagoya University, Nagoya, Japan
Mailing address: Haruo Honjo, MD, Department of Cardiovascular Research, Research Institute of Environmental Medicine, Nagoya University, Furo-cho, Chikusa-ku, Nagoya 464-8601, Japan. E-mail: honjo@riem.nagoya-u.ac.jp

Spiral Wave Reentry in Ventricles

The concept of spiral waves appeared in the generic theory of excitable media to describe rotating waves of excitation in a variety of nonlinear excitable systems of chemical, physical and biological origin[21,22] Winfree is a pioneer who introduced the notion of spiral waves to cardiac electrophysiology to explain the mechanism of functional reentry[4,23,24] In the center of the rotating wave of excitation, the tip of the wave moves along a complex trajectory and waves emanate from the organizing center into the surrounding medium[5–7,10,12,25–28] Because the propagation velocity of a convex wavefront is lower than that of a flat wavefront, as the result of decreased local excitatory current distributing over a relatively larger membrane area downstream (source–sink mismatch), the rotating wave has to acquire the shape of a spiral[3,6,7,10,12,29]

Spiral waves can be initiated when a disruption (wavebreak) of a propagating wave is formed in the excitable medium[3,6,7,9–12,14,30] Interaction of the propagating wavefront with an unexcitable obstacle, which is either an anatomical structure or functionally refractory tissue, results in wavefront fragmentation. The propagation dynamics of a broken wave differ qualitatively from those of planar or circular waves[1–14,23–31] During normal propagation initiated by a linear source (planar wave) or a point source (circular wave), the wavefront of depolarization and the wavetail of repolarization never meet; the distance between them corresponds to the wavelength of excitation. In contrast, in spiral waves, the front and the tail of a propagating wave touch each other at the wavebreak. In this situation, propagation velocity decreases toward the wavebreak (the broken end of the wave), as the result of pronounced source–sink mismatch of local excitatory current, and the wavefront starts to curl. Consequently, the wavebreak serves as a pivot point and the broken wave rotates around this organizing center.

The dynamics and stability of spiral waves in the heart depend on the underlying electrophysiological properties and anatomical structure of the myocardium, and therefore spiral waves can exhibit a variety of phenotypes[3,6,7,9,10,12,14,31–34] It is obvious that stationary spiral waves produce a regular

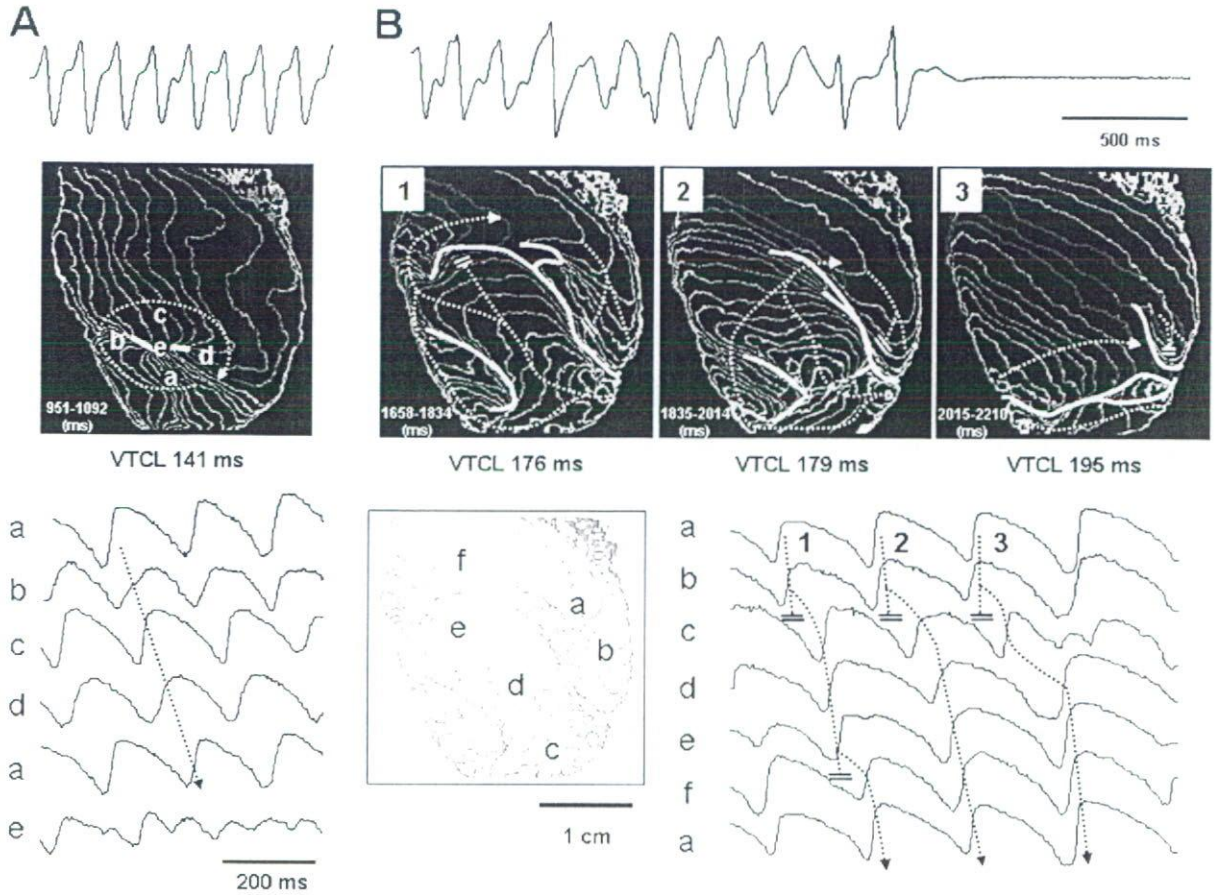

Fig 1. Spiral wave reentry during ventricular tachycardia in the absence (A) and presence (B) of nifekalant (0.1 μmol/L) in 2-dimensional ventricular myocardium of a rabbit heart. (Top) Bipolar electrogram; (Middle) isochrone map of activation (5.33 ms interval) during 1 rotation in control and consecutive 3 rotations after nifekalant; (Bottom) optical action potential signals recorded from 5 sites (a–e) in control and 6 sites (a–f) after nifekalant. Yellow lines in the isochrone maps show functional block (see text for explanation). VTCL, VT cycle length (Reprinted from *Am J Physiol Heart Circ Physiol* 2007; **292:** H539–H548 with permission from the American Physiological Society).

and monomorphic tachycardia pattern. Spiral waves are often anchored to small structural discontinuities, such as vessels, patches of fibrosis tissue, and in these cases, the stationary spiral waves pinned to anatomical structures give rise to long-lasting episodes of monomorphic tachycardia. In contrast, beat-to-beat changes in the organizing center of spiral waves may give rise to a complex pattern of activation, because a drifting spiral wave, like any other moving source of oscillation, produces a Doppler shift in the excitation frequency: the frequency is higher ahead of the moving center and lower behind it. Consequently, when meandering of spiral waves is quasiperiodic, coexisting different excitation frequencies produces the characteristic ECG pattern of TdP, showing waxing and waning modulation. When an organizing center moves at higher speed and in a more irregular and chaotic manner, the ECG pattern becomes more disorganized and loses periodic modulation (characteristic ECG pattern of polymorphic tachycardia or coarse fibrillation). Fibrillation is characterized by a complex spatiotemporal pattern in excitation, which results from spiral wave breakup[8–11,13] (mechanisms of fibrillation maintenance will be described in detail later).

Effects of I_{Kr} Blockade on Spiral Wave Reentry

Spiral Wave Reentry in 2-D Ventricular Myocardium

In the intact ventricular myocardium having considerable wall thickness, functional reentry underlying VT/VF may be represented by scroll waves with a complex 3-dimensional (3-D) appearance rather than 2-D spiral waves.[35–37] However, no experimental methods are currently available for the analysis of wave propagation dynamics in 3-D ventricular myocardium with sufficient detail. Therefore, we created a thin epicardial layer of ventricular muscle preparations (≈1 mm thick) of Langendorff-perfused rabbit hearts by an endocardial cyoablation method originally described by Allessie's group[28,38,39] and propagation of action potentials in a quasi 2-D sheet of the left ventricular free wall was visualized by means of an optical mapping system equipped with a high-speed digital video camera[15–17] (spatial and temporal resolution of the system, 0.1 mm and 1 ms, respectively). In those experiments, motion artifacts were minimized by infusion of an excitation–contraction uncoupler, BDM. The pattern of activation during constant pacing applied around the center of the anterior surface of the left ventricle (LV) exhibited uniform anisotropy: the activation isochromes showed a smooth ellipsoidal pattern with a long

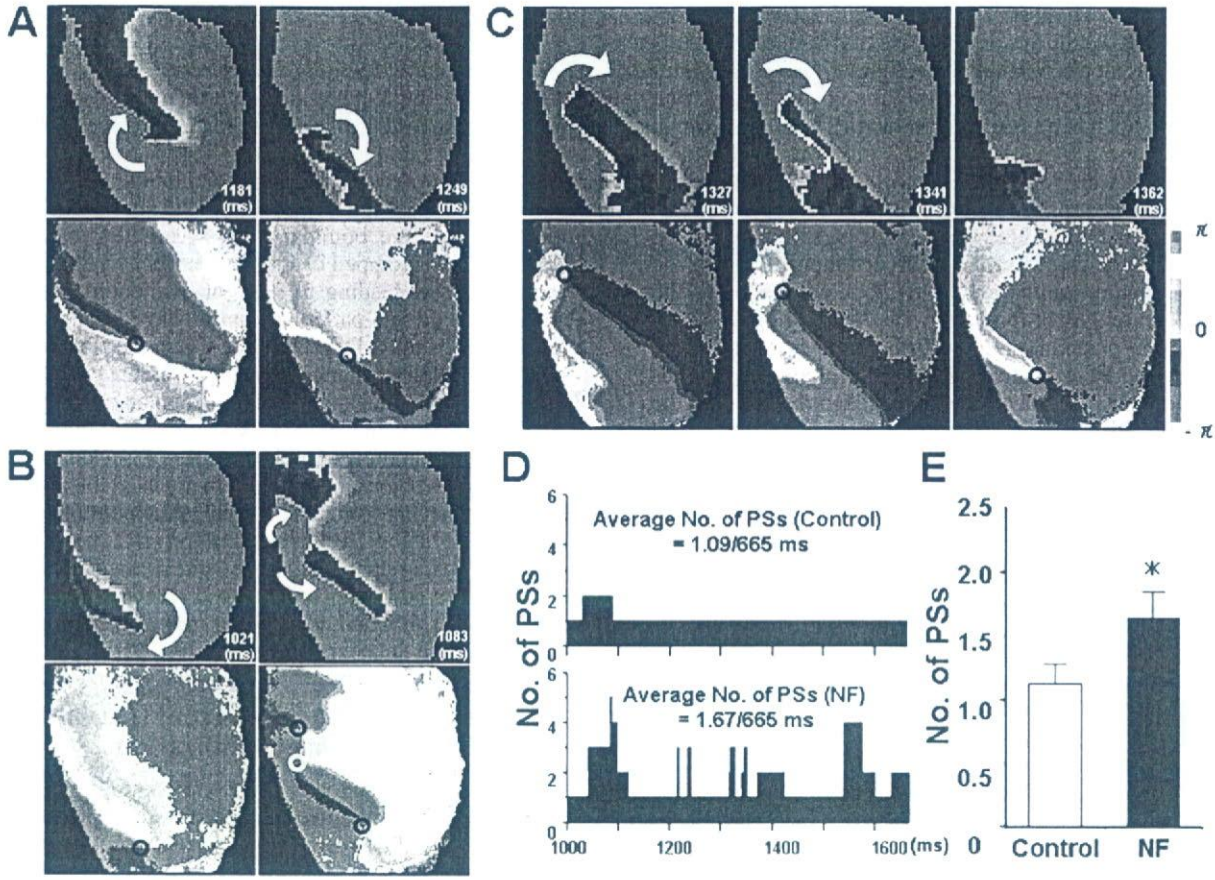

Fig 2. Wavefront-to-tail interactions in spiral wave reentry. (A) In the control, a wavefront (red) and a wavetail (green) do not meet except at the wavebreak (Top panels), which corresponds to a phase singularity (PS, black open circle in bottom panels). (B,C) Interactions between a wavefront and a wavetail result in either formation of a pair of counter-rotating PSs (B) or a sudden spatial jump of the original PS (C) in the presence of nifekalant (0.1 μmol/L). (●) PS of clockwise rotation. (○) PS of counter-clockwise rotation. (D) Time course of changes in the number of PSs in the observation area during ventricular tachycardia before (Control) and after nifekalant (NF). E, summarized data for the average number of PSs (for 655 ms) before (Control) and after nifekalant (NF) (means ± SD, n=7. *p<0.05) (Reprinted from *Am J Physiol Heart Circ Physiol* 2007; **292**: H539–H548 with permission from the American Physiological Society)

axis almost parallel to the myocardial fiber orientation. The anisotropic ratio of conduction velocity estimated around the central area of the LV free wall was 2.4–2.6[15–17] A pair of paddle electrodes was placed on the lateral surface of both ventricles, and a single monophasic DC pulse (20 V, 10 ms) was applied to the heart during a vulnerable period of preceding constant stimuli from the apex. This "modified cross-field" stimulation consistently induced self-terminating or sustained VT. In approximately 60% of these VT episodes, a single-loop or figure-of-eight pattern of spiral wave reentry was documented and, in the remaining VTs, one-way propagation of excitation waves was observed[15–17] There was no breakthrough pattern of activation during any of the VT episodes induced by modified cross-field stimulation, suggesting that neither focal activity (enhanced automaticity and triggered activity) nor transmural reentry is responsible for the occurrence of VT in the quasi-2D ventricular preparations[15–17]

Effects of Nifekalant on Spiral Wave Dynamics

The effects of nifekalant (0.1 μmol/L) on the action potential and conduction have been characterized during constant pacing at a cycle length of 200–800 ms[15–17] Nifekalant prolongs the action potential duration (APD) in a reverse-frequency dependent manner (by 7–25%) without affecting conduction velocity. The APD prolongation was spatially homogeneous in the LV, but APD alternans during rapid pacing was enhanced after nifekalant. Nifekalant increased the maximum slope of APD restitution curves (from 0.48 to 0.70), but the values did not exceed 1 even after nifekalant administration. This suggests that factors other than restitution properties, such as unstable Ca^{2+} dynamics, electrotonic currents and short-term memory, may be also involved in the increased dynamic instability (APD alternans) induced by nifekalant. Cross-field stimulation induced VT in the presence of nifekalant, as in the control group, but the VT duration was significantly shorter after nifekalant: the percentage of sustained VT (>30 s) in the total VT episodes was approximately 20% under control conditions and was decreased to approximately 4% after nifekalant, and most VTs (>80%) self-terminated within 5 s after induction in the presence of nifekalant.

Fig 1A is a representative record of spiral wave reentry during a VT episode under control conditions: a spiral wave is rotating around a short line of functional block (≈7 mm in length) and this pattern of activation was stable for more than 10 s[17] The distant bipolar electrogram of ventricular excitation during this VT episode shows a monomorphic

pattern. Optical membrane potential signals recorded from the line of block show a double-potential pattern, which is characteristic of electrotonic interaction of excitation waves with a large phase shift across the line. This suggests that the line of block is a result of a refractory wake of a single wave moving back and forth after a full turn at the end of the line. According to the original theoretical concept of spiral wave reentry in an excitable media, the core of the spiral is excitable but unexcited. However, this is not the case in the real 2-D ventricular myocardium. Instead, the wave is rotating around a line of block equivalent to the "inactive core", as proposed by the "leading circle" concept. Action potential signals close to the pivot point are characterized by a prolonged upstroke phase, sometimes with a notch, which may reflect a localized reduction in the excitatory current at the pronounced convex wavefront close to the pivot point.

Spiral wave reentry induced after application of nifekalant is not stationary but shows irregular meandering along remarkably prolonged complex lines of functional block (Fig 1B)[17] Most lines of functional block are the result of a refractory wake of preceding excitations, similar to those under control conditions but, when multiple waves coexist (see the next section), head-on collision of wavefronts also produces lines of functional block. The electrogram shows a polymorphic pattern of VT with varying cycle length. Optical action potential signals also show a large beat-to-beat change in morphology. Such disorganized spiral wave reentry in the presence of nifekalant could not be sustained and self-terminated.

Interactions Between Wavefront and Wavetail

The nifekalant-induced modification of spiral wave reentry can be further characterized in terms of the wavefront–wavetail interaction and the phase singularity dynamics (Fig 2)[17] In spiral wave reentry under control conditions, the wavefront of depolarization is always chasing its own tail of repolarization and they rarely met each other, except at the tip of the wave. Therefore, the number of phase singularities (the organizing center of a spiral wave) recognized in the phase map is normally 1 (a single rotor) and only transiently increases to 2. After administration of nifekalant, the wavefront frequently encounters its own tail at the spiral arm distant from the tip of the spiral wave. Such interactions of the wavefront and the wavetail result in either breakup of the original wave or a sudden movement of the organizing center of the spiral wave. In the phase map, the former is recognized as the appearance of a pair of new phase singularities with opposite chirality and the latter as a sudden spatial jump of the original phase singularity. Both of these events result in a remarkable enhancement of the disorganization of the spiral wave dynamics and prevention of their pinning to anatomical structures.

Theoretical studies have proposed 2 different mechanisms of spiral wave breakup in homogeneous tissue[27,33]: one is the result of large meandering of the spiral tip, producing prominent dispersion of the wavelength, leading to complex spatiotemporal chaos; the other type of breakup occurs in response to enhanced alternans of the wavelength in the spiral arm at a certain distance from a relatively stable organizing center. In the latter case, the dominant periodicity of excitation is kept constant. The spiral wave breakup in the presence of nifekalant may be attributable mainly to the former mechanism, because the breakup is associated with large meandering and marked variation of excitation cycle length.

Self-Termination of Spiral Wave Reentry

Computer simulation studies and theoretical considerations have suggested that there are 3 different modes of termination of spiral wave reentry[40]: (1) a pair of counter-rotating spiral waves can mutually annihilate via collision of their rotation centers; (2) a spiral wave can run off a nonexcitable tissue boundary and terminate; and (3) a spiral wave tip is trapped in a region entirely surrounded by refractory tissue, leading to its own extinction. We have demonstrated these 3 patterns of spiral wave termination in experiments using 2-D ventricular tissue of rabbit hearts with the aid of phase mapping analysis[17] In the control conditions, type 1 (mutual annihilation of counter-rotating spiral waves) was the major mode of spontaneous termination of spiral waves. In contrast, in the presence of nifekalant, type 2 (collision of a phase singularity with nonexcitable tissue in the atrioventricular groove) and type 3 (trapping of a phase singularity in a region surrounded by refractory tissue) modes are predominant in spiral wave self-termination. The former may be the result of enhanced meandering and unpinning of the spiral tip and the latter may be a consequence of repolarization delay and its beat-to-beat variation.

Inward Rectifier K+ Current (I_{K1}) and Spiral Wave Stabilization

In working cardiomyocytes, action potential repolarization depends on coordinated activation of multiple types of K+ currents: delayed rectifier K+ currents (I_{Kr}, I_{Ks}), transient outward current (I_{to}), and I_{K1}. During spiral wave propagation, the contribution of respective K+ currents is considered to be spatially heterogeneous, depending on their vicinity to the spiral tip[41–43] The results of our optical mapping study have suggested that I_{Kr} plays a significant role in action potential repolarization close to the spiral tip, because the selective blockade of this current by nifekalant enhanced meandering of the spiral tip. Such destabilization of spiral waves promotes their self-termination. A recent computer simulation study, using the Luo-Rudy action potential model, has also demonstrated that blockade of the delayed rectifier K+-channel increases dynamic instability and promotes spiral wave extinction through mutual annihilation and collision with an anatomical boundary in a finite-sized 2-D sheet[44] In contrast, Jalife et al[41–43] have proposed that instantaneous I_{K1}, rather than time-dependent I_K, is the major repolarizing current responsible for the prematurely abbreviated wavetail close to the spiral tip. In their studies using guinea-pig hearts, spatiotemporal periodicities with a domain-like distribution of excitation frequency always exist during VF and a persistent stable rotor that provides exceedingly high-frequency excitation and fibrillatory conduction is consistently located in the LV where the outward component of I_{K1} is larger than that in the right ventricle[42,43] Selective blockade of I_{K1} by Ba^{2+} was shown to abolish the high-frequency excitation in the LV and facilitate self-termination of VF[45] They have also demonstrated recently that genetic overexpression of Kir2.1, a major pore-forming unit of the I_{K1} channel, in the mouse heart results in a remarkable increase in the VF/VT frequency and a significant prolongation of VF/VT duration[46] Based on those findings they have argued that I_{K1} plays a key role in action potential repolarization close to the spiral tip, allowing high-frequency rotors to stabilize[43]

VF and K+-Channel Blockade

As for the role of spiral-wave reentry in the maintenance of VF, there are 2 major working hypotheses: a "multiple-wavelet" hypothesis and a "mother rotor" hypothesis, in which the role of spiral wave breakup differs.[10,42,43,47–50] According to the multiple-wavelet hypothesis, continuously generated wavebreak is the engine maintaining VF. In this hypothesis, wave breakup is originally thought to be the result of structural and/or functional heterogeneity of the myocardium, but it has been recently emphasized that dynamic factors, such as restitution properties, play synergistic roles with preexisting heterogeneity in amplifying the wave instability leading to spiral wave breakup ("dynamic wavebreak hypothesis").[11,48,49] On the other hand, Jalife et al have proposed that a fairly stable mother rotor serves as a source of high-frequency excitation and, because of its high frequency rate, waves of excitation emanating from the rotor develop intermittent conduction block at the periphery (fibrillatory conduction), which gives rise to the characteristic complex pattern of QRS on the ECG.[10,42,43,50] Therefore, in this theory, wavebreak is just an epiphenomenon and not essential for the maintenance of VF. Recent studies have shown that these 2 mechanisms are interchangeable, depending on underlying conditions.[51–53]

Mother-rotor-type VF will not self-terminate as long as the mother rotor is anchored to small structural discontinuities.[54] Blockade of I_{Kr} promotes meandering and breakup of spiral waves through an increase in dynamic instability, and this facilitates unpinning of the spiral waves from anatomical structures.[17,55,56] Unstable spiral waves showing chaotic meandering tend to self-terminate as a result of collision of the spiral tip with the nonexcitable boundary of a limited area of tissue. These processes may explain, in part, the antiarrhythmic actions of I_{Kr} blockers. Blockade of I_{K1} may have similar actions. In contrast, the increased spiral wave breakup by I_{Kr} blockade, as a result of increased wavefront–wavetail interactions in the spiral arm, promotes degeneration of stable VT to complex multiple wavelet-type VF, and this may be involved in the profibrillatory actions of I_{Kr} blockers. Such actions might be less with I_{K1} blockade, if the relative contribution of I_{K1} to action potential repolarization is much greater in the vicinity of the spiral tip than in the spiral arm. As for the modification of spiral wave reentry dynamics by K+-channel blockade, information available to date is mainly from 2-D cardiac tissues in computer simulation or in real hearts of small animals. Extending these results to 3-D hearts, especially in larger animals including humans, is not straightforward. An increase in the tissue mass (surface area and wall thickness) would reduce the chance of spontaneous termination of spiral wave reentry by rotor collision or trapping, and it would enhance rotor meandering and wave instability through complex 3-D dynamics in favor of the transition from VT to VF. The greater structural discontinuities and functional heterogeneities in diseased hearts would also alter the spatial requirements of spontaneous rotor termination. Further experimental and theoretical studies are required to shed light on these issues.

Acknowledgments

This study was supported, in part, by a Grant-in-Aid for Scientific Research (C) from the Ministry of Health, Labour and Welfare and from the Suzuken Memorial Foundation.

References

1. Davidenko JM, Kent PF, Chialvo DR, Michaels DC, Jalife J. Sustained vortex-like waves in normal isolated ventricular muscle. *Proc Natl Acad Sci USA* 1990; **7:** 8785–8789.
2. Davidenko JM, Pertsov AV, Salomonsz R, Baxter W, Jalife J. Stationary and drifting spiral waves of excitation in isolated cardiac muscle. *Nature* 1992; **355:** 349–351.
3. Pertsov AM, Davidenko JM, Salomonsz R, Baxter WT, Jalife J. Spiral waves of excitation underlie reentrant activity in isolated cardiac muscle. *Circ Res* 1993; **72:** 631–650.
4. Winfree AT. Electrical turbulence in three-dimensional heart muscle. *Science* 1994; **266:** 1003–1006.
5. Gray RA, Jalife J, Panfilov AV, Baxter WT, Cabo C, Davidenko JM, et al. Mechanisms of cardiac fibrillation. *Science* 1995; **270:** 1222–1223.
6. Davidenko JM. Spiral waves in the heart: Experimental demonstration of a theory. *In*: Zipes DP, Jalife JJ, editors. Cardiac electrophysiology: From cell to bedside, 2nd edn. Philadelphia: WS Saunders; 1995; 478–488.
7. Fast VG, Kléber AG. Role of wavefront curvature in propagation of cardiac impulse. *Cardiovasc Res* 1997; **33:** 258–271.
8. Gray RA, Pertsov AM, Jalife J. Spatial and temporal organization during cardiac fibrillation. *Nature* 1998; **392:** 75–78.
9. Weiss JN, Garfinkel A, Karagueuzian HS, Qu Z, Chen PS. Chaos and the transition to ventricular fibrillation: A new approach to antiarrhythmic drug evaluation. *Circulation* 1999; **99:** 2819–2826.
10. Jalife J. Ventricular fibrillation: Mechanisms of initiation and maintenance. *Annu Rev Physiol* 2000; **62:** 25–50.
11. Weiss JN, Chen PS, Qu Z, Karagueuzian HS, Garfinkel A. Ventricular fibrillation: How do we stop the waves from breaking? *Circ Res* 2000; **87:** 1103–1107.
12. Kléber A, Janse MJ, Fast VG. Normal and abnormal conduction in the heart. *In*: The handbook of physiology: The cardiovascular system. Bethesda: Oxford University Press; 2001; 455–530.
13. Tung L, Bursac N, Aguel F. Rotors and spiral waves in two dimensions. *In*: Zipes DP, Jalife J, editors. Cardiac electrophysiology: From cell to bedside, 4th edn. Philadelphia: WS Saunders; 2004; 336–344.
14. Weiss JN, Qu Z, Chen PS, Lin SF, Karagueuzian HS, Hayashi H, et al. The dynamics of cardiac fibrillation. *Circulation* 2005; **112:** 1232–1240.
15. Amino M, Yamazaki M, Nakagawa H, Honjo H, Okuno Y, Yoshioka K, et al. Combined effects of nifekalant and lidocaine on the spiral-type re-entry in a perfused 2-dimensional layer of rabbit ventricular myocardium. *Circ J* 2005; **69:** 576–584.
16. Kodama I, Honjo H, Yamazaki M, Nakagawa H, Ishiguro Y, Okuno Y, et al. Optical imaging of spiral waves: Pharmacological modification of spiral-type excitations in a 2-dimensional layer of ventricular myocardium. *J Electrocardiol* 2005; **38**(Suppl): 126–130.
17. Yamazaki M, Honjo H, Nakagawa H, Ishiguro YS, Okuno Y, Amino M, et al. Mechanisms of destabilization and early termination of spiral wave reentry in the ventricle by a class III antiarrhythmic agent, nifekalant. *Am J Physiol Heart Circ Physiol* 2007; **292:** H1539–H548.
18. Myoishi M, Yasuda S, Miyazaki S, Ueno K, Morii I, Satomi K, et al. Intravenous administration of nifekalant hydrochloride for the prevention of ischemia-induced ventricular tachyarrhythmia in patients with renal failure undergoing hemodialysis. *Circ J* 2003; **67:** 898–900.
19. Yoshioka K, Amino M, Morita S, Nakagawa Y, Usui K, Sugimoto A, et al. Can nifekalant hydrochloride be used as a first-line drug for cardiopulmonary arrest (CPA)?: Comparative study of out-of-hospital CPA with acidosis and in-hospital CPA without acidosis. *Circ J* 2006; **70:** 21–27.
20. Roden DM. Drug-induced prolongation of the QT interval. *N Engl J Med* 2004; **350:** 1013–1022.
21. Winfree AT. Spiral waves of chemical activity. *Science* 1972; **175:** 634–635.
22. Winfree AT. Scroll-shaped waves of chemical activity in three dimensions. *Science* 1973; **181:** 937–939.
23. Winfree AT. Electrical instability in cardiac muscle: Phase singularities and rotors. *J Theor Biol* 1989; **138:** 353–405.
24. Winfree AT. Theory of spirals. *In*: Zipes DP, Jalife J, editors. Cardiac electrophysiology: From cell to bedside, 2nd edn. Philadelphia: WS Saunders; 1995; 378–389.
25. Karma A. Electrical alternans and spiral wave breakup in cardiac tissue. *Chaos* 1994; **4:** 461–472.
26. Courtemanche M. Complex spiral wave dynamics in a spatially distributed ionic model of cardiac electrical activity. *Chaos* 1996; **6:** 579–600.

27. Qu Z, Xie F, Garfinkel A, Weiss JN. Origins of spiral wave meander and breakup in a two-dimensional cardiac tissue model. *Ann Biomed Eng* 2000; **28:** 755–771.
28. Schalij MJ, Boersma L, Huijberts M, Allessie MA. Anisotropic reentry in a perfused 2-dimensional layer of rabbit ventricular myocardium. *Circulation* 2000; **102:** 2650–2658.
29. Cabo C, Pertsov AM, Baxter WT, Davidenko JM, Gray RA, Jalife J. Wave-front curvature as a cause of slow conduction and block in isolated cardiac muscle. *Circ Res* 1994; **75:** 1014–1028.
30. Cabo C, Pertsov AM, Davidenko JM, Baxter WT, Gray RA, Jalife J. Vortex shedding as a precursor of turbulent electrical activity in cardiac muscle. *Biophys J* 1996; **70:** 1105–1111.
31. Gray RA, Jalife J, Panfilov A, Baxter WT, Cabo C, Davidenko JM, et al. Nonstationary vortexlike reentrant activity as a mechanism of polymorphic ventricular tachycardia in the isolated rabbit heart. *Circulation* 1995; **91:** 2454–2469.
32. Garfinkel A, Qu Z. Nonlinear dynamics of excitation and propagation in cardiac muscle. *In*: Zipes DP, Jalife J, editors. Cardiac electrophysiology: From cell to bedside, 3rd edn. Philadelphia: WS Saunders; 2000; 315–320.
33. Fenton FH, Cherry EM, Hastings HM, Evans SJ. Multiple mechanisms of spiral wave breakup in a model of cardiac electrical activity. *Chaos* 2002; **12:** 852–892.
34. Qu Z, Garfinkel A. Nonlinear dynamics of excitation and propagation in cardiac muscle. *In*: Zipes DP, Jalife J, editors. Cardiac electrophysiology: From cell to bedside, 4th edn. Philadelphia: WS Saunders; 2004; 327–335.
35. Pertsov AM, Jalife J. Scroll waves in three-dimensional cardiac muscle. *In*: Zipes DP, Jalife JJ, editors. Cardiac electrophysiology: From cell to bedside, 2nd edn. Philadelphia: WS Saunders; 1995; 403–410.
36. Efimov IR, Sidorov V, Cheng Y, Wollenzier B. Evidence of three-dimensional scroll waves with ribbon-shaped filament as a mechanism of ventricular tachycardia in the isolated rabbit heart. *J Cardiovasc Electrophysiol* 1999; **10:** 1452–1462.
37. Wellner M, Berenfeld O, Jalife J, Pertsov AM. Minimal principle for rotor filaments. *Proc Natl Acad Sci USA* 2002; **99:** 8015–8018.
38. Schalij MJ, Lammers WJ, Rensma PL, Allessie MA. Anisotropic conduction and reentry in perfused epicardium of rabbit left ventricle. *Am J Physiol Circ Physiol* 1992; **263:** H1466–H1478.
39. Danse PW, Garratt CJ, Allessie MA. Flecainide widens the excitable gap at pivot points of premature turning wavefronts in rabbit ventricular myocardium. *J Cardiovasc Electrophysiol* 2001; **12:** 1010–1017.
40. Qu Z. Critical mass hypothesis revisited: Role of dynamical wave stability in spontaneous termination of cardiac fibrillation. *Am J Physiol Heart Circ Physiol* 2006; **290:** H255–H263.
41. Beaumont J, Jalife J. Rotors and spiral waves in two dimensions. *In*: Zipes DP, Jalife J, editors. Cardiac electrophysiology: From cell to bedside, 3rd edn. Philadelphia: WS Saunders; 2000; 327–335.
42. Samie FH, Berenfeld O, Anumonwo J, Mironov SF, Udassi S, Beaumont J, et al. Rectification of the background potassium current: A determinant of rotor dynamics in ventricular fibrillation. *Circ Res* 2001; **89:** 1216–1223.
43. Samie FH, Jalife J. Mechanisms underlying ventricular tachycardia and its transition to ventricular fibrillation in the structurally normal heart. *Cardiovasc Res* 2001; **50:** 242–250.
44. Warren M, Guha PK, Berenfeld O, Zaitsev A, Anumonwo JM, Dhamoon AS, et al. Blockade of the inward rectifying potassium current terminates ventricular fibrillation in the guinea pig heart. *J Cardiovasc Electrophysiol* 2003; **14:** 621–631.
45. Qu Z, Weiss JN. Effects of Na^+ and K^+ channel blockade on vulnerability to and termination of fibrillation in simulated normal cardiac tissue. *Am J Physiol Heart Circ Physiol* 2005; **289:** H1692–H1701.
46. Noujaim SF, Pandit SV, Berenfeld O, Vikstrom K, Cerrone M, Mironov S, et al. Up-regulation of the inward rectifier K^+ current (I_{K1}) in the mouse heart accelerates and stabilizes rotors. *J Physiol* 2007; **578:** 315–326.
47. Riccio ML, Koller ML, Gilmour RF Jr. Electrical restitution and spatiotemporal organization during ventricular fibrillation. *Circ Res* 1999; **84:** 955–963.
48. Garfinkel A, Kim YH, Voroshilovsky O, Qu Z, Kil JR, Lee MH, et al. Preventing ventricular fibrillation by flattening cardiac restitution. *Proc Natl Acad Sci USA* 2000; **97:** 6061–6066.
49. Weiss JN, Chen PS, Qu Z, Karagueuzian HS, Lin SF, Garfinkel A. Electrical restitution and cardiac fibrillation. *J Cardiovasc Electrophysiol* 2002; **13:** 292–295.
50. Chen J, Mandapati R, Berenfeld O, Skanes AC, Jalife J. High-frequency periodic sources underlie ventricular fibrillation in the isolated rabbit heart. *Circ Res* 2000; **86:** 86–93.
51. Wu TJ, Lin SF, Weiss JN, Ting CT, Chen PS. Two types of ventricular fibrillation in isolated rabbit hearts: Importance of excitability and action potential duration restitution. *Circulation* 2002; **106:** 1859–1866.
52. Chen PS, Wu TJ, Ting CT, Karagueuzian HS, Garfinkel A, Lin SF, et al. A tale of two fibrillations. *Circulation* 2003; **108:** 2298–2303.
53. Wu TJ, Lin SF, Baher A, Qu Z, Garfinkel A, Weiss JN, et al. Mother rotors and the mechanisms of D600-induced type 2 ventricular fibrillation. *Circulation* 2004; **110:** 2110–2118.
54. Starmer CF, Romashko DN, Reddy RS, Zilberter YI, Starobin J, Grant AO, et al. Proarrhythmic response to potassium channel blockade: Numerical studies of polymorphic tachyarrhythmias. *Circulation* 1995; **92:** 595–605.
55. Ripplinger CM, Krinsky VI, Nikolski VP, Efimov IR. Mechanisms of unpinning and termination of ventricular tachycardia. *Am J Physiol Heart Circ Physiol* 2006; **291:** H184–H192.
56. Hua F, Gilmour RF Jr. Contribution of I_{Kr} to rate-dependent action potential dynamics in canine endocardium. *Circ Res* 2004; **94:** 810–819.

日本心電学会誌

心電図

Japanese Journal of Electrocardiology

Volume 27 Number 4 2007

総　説

薬物による心室スパイラル・リエントリーの制御
—K^+チャネル遮断薬の有用性と限界—

児玉逸雄*　本荘晴朗*　山崎正俊*　原田将英*
石黒有子*　高成広起*　神谷香一郎*

心臓突然死の主要な原因である心室頻拍・細動(VT/VF)の成立には，渦巻き型の旋回興奮(スパイラル・リエントリー)が重要な役割を果たすことが知られている．薬物によるスパイラル・リエントリーの制御に関しては，従来はコンピュータシミュレーションを用いた検討が主体であり，実験的な検証は不十分であった．最近われわれは，小動物の灌流心標本を用いた活動電位光学マッピング実験で，遅延整流K^+チャネル電流の速い活性化成分(I_{Kr})を遮断する薬物が，心室に誘発したスパイラル・リエントリーを不安定にするだけでなく，その早期停止を促す作用があることを発見した．前者は多形性のVTからVFへの移行をもたらす危険性(催不整脈作用)を意味しており，後者はVT/VFの停止を促す作用(抗不整脈作用)の基盤となる．本稿では，K^+チャネル遮断薬のもつこの二面性を解説する

(心電図，2007；27：275～286)

Ⅰ．はじめに

心室の頻脈性不整脈(頻拍・細動：VT/VF)は血行動態の破綻をきたし，心臓突然死の主要な原因となる．近年，これらの不整脈の成立に機能的な障害物の周囲を旋回する渦巻き型興奮(スパイラル・リエントリー)が重要な役割を果たすことが示され，それらの不整脈を制御するうえでの新しい概念として注目を集めている[1)～4)]．スパイラル・リエントリーを薬物で制御することが可能であれば，不整脈による死亡を大幅に減らす手段となる．心室におけるスパイラル・リエントリーのダイナミクスに対する薬物の作用に関しては，従来はコンピュータシミュレーションを用いた検討が主体であり，実験的な検証は不十分であった．最近われわれは，ウサギの二次元灌流心標本を用いた活動電位光学マッピング実験で，遅延整流K^+チャネル電流の速い活性化成分(I_{Kr})を遮断するニフェカラントが，心室に誘発したスパイラル・リエントリーを不安定にするだけでなく，その早期停止を促す作用があることを発見した[5)～7)]．

Keywords
- 心室頻拍・細動
- スパイラル・リエントリー
- K^+チャネル遮断薬
- 活動電位光学マッピング

＊名古屋大学環境医学研究所 心・血管分野
(〒464-8601　名古屋市千種区不老町)

Pharmacological regulation of spiral wave reentry in the ventricle : Benefits and limitations of K channel blockers
Itsuo Kodama, Haruo Honjo, Masatoshi Yamazaki, Masahide Harada, Yuko Ishiguro, Hiroki Takanari, Kaichiro Kamiya

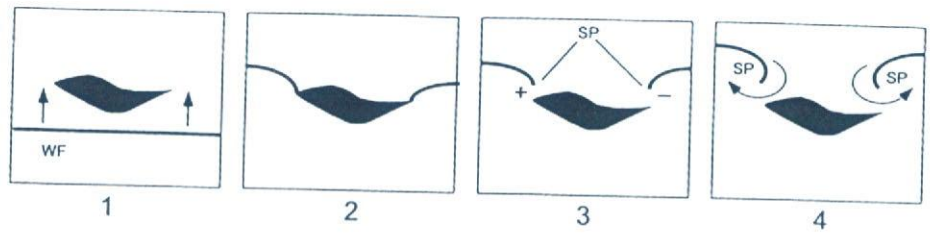

図1　スパイラル興奮波の形成

興奮波の進行方向に障害物(瘢痕組織や不応期の残存)があると，障害物によって興奮波の端が切れた状態(wavebreak：WB)ができ，そこから興奮前面の彎曲が始まり，スパイラル興奮が形成される．

〔文献1)より引用改変〕

我が国で開発されたⅢ群抗不整脈薬のニフェカラントには，治療に難渋するVT/VFへの有効性や，心肺蘇生時の救命効果を高める作用があることが報告されている[8)~12)]．心筋のK^+チャネル遮断は，心室再分極の遅延と心電図のQT延長からTorsades de Pointes(TdP)型の多形性VTやVFをもたらす危険性があるが[13)]，一方ではVT/VFを停止させる作用も有している．本稿では，K^+チャネル遮断薬のもつこの二面性をスパイラル・リエントリーのダイナミクス制御の面から解説するとともに，今後のVT/VF治療戦略における役割について考察してみたい．

Ⅱ．スパイラル・リエントリー

スパイラル・リエントリーは，コンピュータシミュレーションから提唱された概念であり，特定の解剖学的経路をもたず，一拍ごとに旋回経路が変化する機能的リエントリーである．1990年ごろから膜電位感受性色素を用いた活動電位の光学マッピング実験で，その実態が観察できるようになった[1), 2)]．スパイラル・リエントリーの成立には，興奮波の端が途切れる現象(wavebreak)と，興奮前面の彎曲(curvature)が伝導に及ぼす影響を考える必要がある[1), 2), 14)]．心臓の中を進む興奮波が，先行興奮の不応期がまだ残っている領域や，梗塞巣，瘢痕などの障害物にぶつかると，興奮波の端が途切れて，興奮前面に彎曲ができる(図1)[1)]．この彎曲は，端に向かうにつれて大きくなるため興奮の下流(未興奮部位)に対する上流(既興奮部位)の比率がしだいに小さくなり，興奮前面に発生する局所電流の刺激効率が減少して，伝導速度の低下に至る．興奮波の端では，興奮前面が再分極終末とぶつかって，伝導速度が0となる特異点(q)が形成される．そして，興奮波は，この特異点を中心として螺旋(スパイラル)を描いて旋回し続けることになる(図2)[14)]．スパイラルの旋回中心は，コマの回転軸が移動するように，多かれ少なかれ，さまよい運動(meandering)を起こす．またスパイラルが複数に分裂して，全体の統制が失われたように見えることもある．スパイラル・リエントリーは，興奮前面のダイナミックな変化をきっかけにして発生する現象であり，不応期や伝導性，興奮性の恒常的な不均一性を必ずしも必要としない(正常心臓でも発生する)．しかし，これらの不均一性があれば，スパイラルのきっかけとなるwavebreakやcurvatureが発生しやすくなる．

図3は，心室スパイラル・リエントリーのダイナミクスと，その表現形である心電図波形・不整脈との関係を示す[15)]．スパイラル興奮の旋回中心が狭い領域にとどまって安定した旋回が続く場合，心電図波形は単形性の心室頻拍(monomorphic VT)となる．心筋組織には線維走行の変化，血管，結合組織などによる様々な不連続性があり，スパイラル興奮波の断端(旋回中心)は，それらの不連続構造に投錨(anchoringもしくはpinning)する性質を有する[30)]．スパイラルの旋回中心が，ある程度以上大きくなり，周期的なmeanderingを示すようになると，旋回周

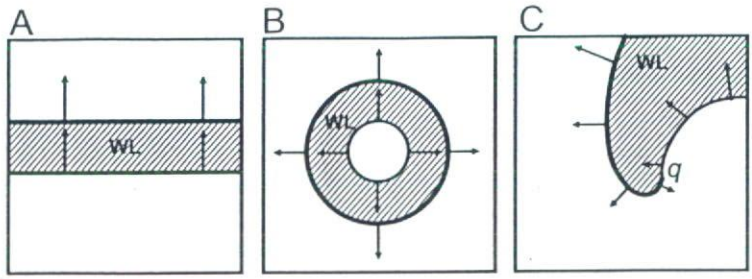

図2　三種類の興奮波

A：直線的な興奮波(planar wave).
B：中心から周辺へと広がる円形の興奮波(circular wave).
C：スパイラル型興奮波(spiral wave). 太い実線は興奮前面，斜線の部分は興奮波長(wave length, WL)に相当する脱分極領域を示す. Spiral waveでは，興奮前面と再分極終末が一致する特異点(q)が形成される.
〔文献14)より引用改変〕

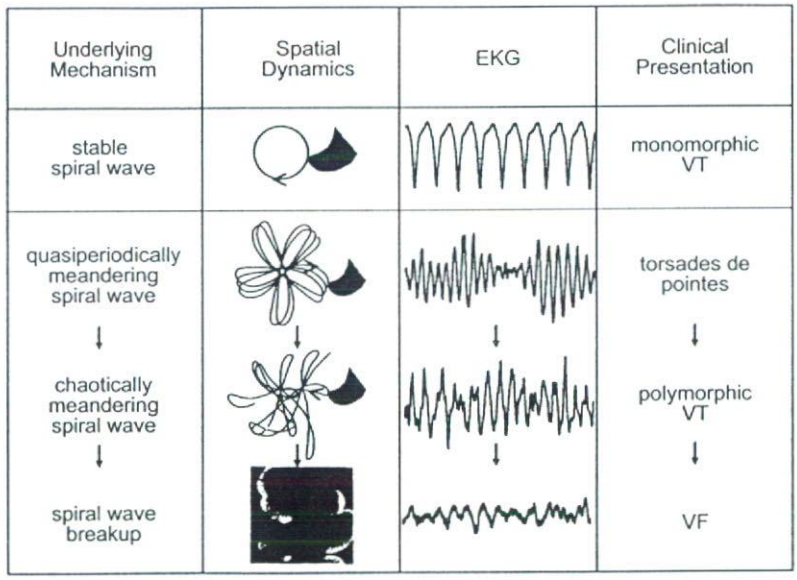

図3　心室スパイラル・リエントリーのダイナミクスと心電図・不整脈
〔文献15)より引用改変〕

期もそれに対応して変動する．この場合，心電図波形はQRS軸がねじれたようなTdPとなる．さまよい運動がさらに大きく，無秩序になると，興奮周期の変動は一層複雑化し，多形性心室頻拍(polymorphic VT)あるいは粗い心室細動(coarse VF)を引き起こす．スパイラル興奮波の旋回中心から離れた領域で，興奮前面と再分極終末の相互作用が生ずると，スパイラルは分裂し(breakup)，そこから新たな興奮波が発生する．このような機序により興奮波の生成と消滅を繰り返す状態では，心電図波形はVFを呈する[15), 16)].

ただし，VFの成立には，上記のような興奮波の動的不安定性による分裂と生成が本質的な役割を果たすとする"動的興奮波分裂(dynamic wavebreak)仮説"とは別に，周期の短い単一あるいは少数のスパイラル・リエントリーが安定して存在し，そこか

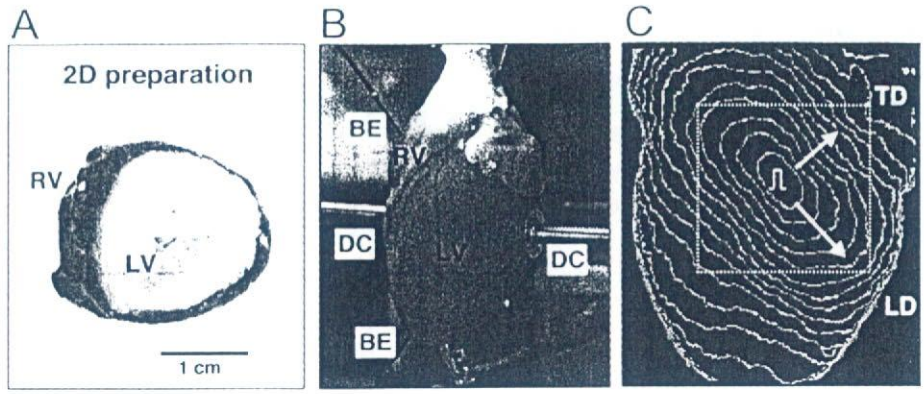

図4　ウサギ心臓の二次元灌流標本と異方性伝導特性(anisotropic conduction property)

A：心内膜側を凍結凝固して作製した二次元心外膜下心筋組織(2,3,5-triphenyltetrazolium chloride：TTC染色)．

B：心内膜側を凍結凝固した後，膜電位光学マッピング用にLangendorff灌流装置に設置した心臓．DCは直流通電用の円盤電極，BEは心電図記録用の遠隔双極電極を示す．

C：基本刺激下(BCL 800 ms)の興奮伝播等時線図(2.67 ms間隔)．中央の正方形(破線)は興奮伝導速度と活動電位持続時間の計測領域を示す(LDは心筋線維走行に沿った方向，TDはそれを横切る方向を現す)．

ら遠心性に伝播する興奮波が心筋特性(とくに不応期)の不均一性に遭遇して複雑にブロックされることにより細動様の伝播(fibrillatory conduction)を示すためとする"マザーローター(mother rotor)仮説"も提唱されている[17-19]．

Ⅲ．ニフェカラント(I_{Kr}遮断薬)の作用

1．二次元灌流標本の活動電位光学マッピング

心室壁には厚みがあるため，そこに発生したスパイラル・リエントリーは実際には三次元構造(スクロールとよばれる)をとり，点ではなくリボン状の旋回中心(フィラメント)をもつ．このフィラメントは形状が複雑に変化する．したがって，心表面には渦巻き構造が一瞬現れるが，きわめて不安定であり，すぐにほかの興奮伝播様式に変化してしまう[20-22]．われわれは，心表面上でのスパイラル・リエントリーの観察と薬物作用の解析を容易にするため，ウサギの左室心内膜側を液体窒素で凍結して厚さ1 mmの心外膜下心筋だけを残存させた二次元灌流標本を作製した(図4A，B)[23]．この標本を膜電位感受性色素di-4-ANEPPSで染色し，高輝度発光ダイオード(LED)による光照射で励起した蛍光を，高速デジタルビデオカメラ(Fastcam-Ultima 40K, Photron社製)で撮影・解析した．このシステムは，われわれが東京大学との共同研究で独自に開発した装置であり，時間分解能(1 ms)，空間分解能(0.1 mm)，連続記録時間(10～30 s)のすべての面で，従来のCCDカメラ方式よりも優れており，世界最高水準である．

はじめに，左室前面の中央に刺激電極を置き，伝導特性と活動電位波形に対するニフェカラントの作用を観察した．この基本刺激下(BCL 180～800 ms)では，心筋線維に沿った方向(L方向)に長軸，それを横切る方向(T方向)に短軸をもつ左右対称の楕円形の興奮伝播が観察され，均一な異方向伝導(uniform anisotropic conduction)が確かめられた(図4C)．L方向とT方向の伝導速度比は2.4～2.6であった[7]．ニフェカラント(0.1 μM)は伝導速度に影響を及ぼすことなく，活動電位持続時間(APD)を均一に延長させた(BCL 400 msで16%延長)[7]．APDの回復特性を調べた実験では，ニフェカラントが回

復曲線(restitution curve)の最大傾斜を0.48(コントロール)から0.70まで増大させた[5]．この効果はスパイラル・リエントリーの不安定性を増し，その分裂を促すように作用する[23),24)]．

2．心室頻拍の誘発とスパイラル・リエントリー

VTを誘発する実験では，心尖部の一点から基本刺激(S1, CL 400 ms)を与え，その興奮に直交する方向の単相波電場刺激(S2, 20 V, 10 ms)を心室受攻期に与えた(cross field stimulation)．コントロールでは15羽のウサギ心臓に誘発した93 VT中74 VT(79.6%)が30 s以内に自然停止し(nonsustained)，ほかの19 VT(20.4%)は30 s以上持続した(sustained)[5]．74のnonsustained VT中46 VT(49.5%)が5 s以内に停止した．ニフェカラント作用下では54 VT中52 VT(96.2%)がnonsustainedであり，sustainedは残りの2 VT(3.7%)にすぎなかった．また52のnonsustained VT中44 VT(81.5%)が5 s以内に停止した．ニフェカラント作用下ではVT周期が有意に延長した(188 ± 31 vs. 154 ± 16 ms)[5]．

図5はVT中にスパイラル・リエントリーが観察された実験例の興奮等時線図と旋回経路の活動電位シグナルを示す[5]．コントロール(図5A)では，左室前面のほぼ中央に線状の機能的ブロックライン(FBL, 7 mm)が形成され，その周囲を興奮波が時計方向に旋回している(VT周期は136～141 ms)．この旋回は10 s以上安定して続いた．リエントリーのmeanderingはごくわずかであり，遠隔双極電極で記録した心電図は単形性VTを示した．旋回経路の活動電位シグナルを見ると，いずれも活動電位の再分極の途中から次の活動電位は発生しており，連続する活動電位の電気的拡張期がほとんどない形をしている．FBLの中央では，幅1～2 mmにわたって二峰性電位(double potential)が記録された．

図5Bは，同一標本にニフェカラント(0.1 μM)作用下で誘発した短いVT(3 s)中の興奮パターンを示す[5]．スパイラル・リエントリーは，長い複雑な形状をもつFBL(全体長24～35 mm)の周りを，局所ブロックを示しながら旋回しており，一拍ごとに旋回経路が変化している．VT周期も176～195 msの範囲で変動している．双極誘導心電図はTdP様のpolymorphic VTを示した．旋回中の活動電位シグナルは，著しいmeanderingや，しばしば発生する局所伝導ブロックを反映して，一拍ごとに波形が大きく変動した．他の心臓でも，同様なニフェカラントの作用(FBLの延長，著しいmeandering，スパイラル興奮の早期停止)が観察された[5]．

3．興奮前後面の相互作用と位相特異点の動き

われわれは，ニフェカラントによるスパイラル・リエントリーのダイナミクス変化をさらに詳しく解析するため，front-tail map(興奮前面と再分極終末のみを表示)とphase map(活動電位シグナルを位相に置き換えて表示)を作成した(図6)[5]．コントロールで誘発したVT中は，興奮前面(wave front)はそれ自身の再分極終末(wave tail)を，ある程度の距離(再分極領域)を置いて追いかけているため，frontがtailに衝突することはきわめてまれであった(図6A)．Phase map上の位相特異点(PS)の数は，通常は1(single rotor)であり，ごくまれに短時間だけ2となった．ニフェカラント作用下では，wave frontがしばしばwave tailに衝突してスパイラル興奮が分裂したり(breakup，図6B)，旋回中心がいきなり他の部位へ移動する現象(図6C)が生じた．Phase map上では，前者はPSの増加(1～3)として，後者はPSのジャンプとして表現された．図6Dは，この実験例の観察領域における単位時間(500フレーム，665 ms)当たりのPS数の推移を示す．7例の実験で，PS数の平均値はコントロールの1.13 ± 0.14からニフェカラント作用下では1.63 ± 0.22まで増加した($p < 0.05$)[5]．これらの実験結果は，ニフェカラントにスパイラル・リエントリーのダイナミクスを不安定にし，その分裂を促すとともに，旋回中心が一ヵ所にとどまることを妨げ(抜錨あるいは不定在化：unpinning)，大きなmeanderingをもたらすことを意味している．

4．スパイラル興奮の自然停止

われわれは，コントロールで誘発した10 VTとニ